Available online at www.sciencedirect.com
SCIENCE DIRECT®
Bioorganic & Medicinal Chemistry Letters
ELSEVIER
Bioorganic & Medicinal Chemistry Letters 14 (2004) 1043–1048

Structure based design of a series of potent and selective non peptidic PTP-1B inhibitors

Cheuk K. Lau,[a,*] Christopher I. Bayly,[a,*] Jacques Yves Gauthier,[a] Chun Sing Li,[a] Michel Therien,[a] Ernest Asante-Appiah,[b] Wanda Cromlish,[b] Yves Boie,[b] Farnaz Forghani,[b] Sylvie Desmarais,[b] Qingping Wang,[b] Kathryn Skorey,[b] Deena Waddleton,[b] Paul Payette,[b] Chidambaram Ramachandran,[b] Brian P. Kennedy[b] and Giovana Scapin[c]

[a]*Department of Medicinal Chemistry, Merck Frosst Centre for Therapeutic Research, PO Box 1005, Pointe Claire-Dorval, Quebec H9R 4P8, Canada*
[b]*Department of Biochemistry and Molecular Biology, Merck Frosst Centre for Therapeutic Research, PO Box 1005, Pointe Claire-Dorval, Quebec H9R 4P8, Canada*
[c]*Department of Medicinal Chemistry, Merck Research Laboratories, PO Box 2000, Rahway, NJ 07065, USA*

Received 8 May 2003; accepted 14 November 2003

Abstract—A series of benzotriazole phenyldifluoromethylphosphonic acids were found to be potent PTP-1B inhibitors. Molecular modeling on the X-ray crystal structure of the lead structure led to the design of potent PTP-1B inhibitors that show moderate selectivity against TC-PTP, a very closely related protein tyrosine phosphatase.

Protein tyrosine phosphatase 1B (PTP-1B) has been implicated in the negative regulation of insulin signaling pathway.[1–3] Recent studies showed that PTP-1B knockout mice exhibit increased insulin sensitivity and are resistant to diet-induced obesity.[4] A correlation between insulin resistance states and levels of PTP-1B expression in muscle and adipose tissues in human has been reported.[5–7] Treatment with anti-sense oligonucleotide specific for PTP-1B results in normalization of blood glucose and insulin levels in animal models of type 2 diabetes.[8] These results taken together suggest that PTP-1B may play a role in the insulin resistance associated with diabetes and obesity. Specific PTP-1B inhibitors may thus be therapeutic beneficial in the treatment of these conditions.[9,10]

In the preceding paper, colleagues from our laboratory reported the development of a series of potent and selective non-peptidic PTP-1B inhibitors based on the deoxybenzoin scaffold. This series of compounds is selective for PTP-1B versus a number of other protein tyrosine phosphatases (PTPs) but not against the closely related T cell protein tyrosine phosphatase (TC-PTP). Even though the implication of inhibiting TC-PTP is not yet elucidated, TC-PTP knockout mice are not viable 3–5 weeks after birth.[11] Initial attempts to obtain X-ray crystal structures of PTP-1B complexed with this series of compounds were not successful. Lacking knowledge of how these compounds bind to the active site, it was difficult to design selective inhibitors against TC-PTP. In an attempt to develop a PTP-1B inhibitor that is selective against a broad range of PTPs including TC-PTP, alternative structures based on the deoxybenzoin template were investigated. Herein, we report the development of a series of potent PTP-1B inhibitors based on a tetrasubstituted 4-[2-(1*H*-1,2,3-benzotriazol-1-yl)ethyl]phenyl(difluoro)methyl-phosphonate scaffold. The tetrasubstituted methine structure allowed the exploration of SAR in four directions in space. In addition, X-ray crystal structures of PTP-1B complexed with several compounds in this series were obtained. Molecular modeling based on the structural information obtained from these crystal structures has led to the design of potent PTP-1B inhibitors that exhibit moderate selectivity against TC-PTP. The observed selectivity was corroborated by X-ray crystal structure of the PTP-1B-inhibitor complex.

* Corresponding author. Tel.: +1-514-428-8622; fax: +1-514-428-4900; e-mail: lau@merck.com; christopher_bayly@merck.com

0960-894X/$ - see front matter © 2004 Elsevier Ltd. All rights reserved.
doi:10.1016/j.bmcl.2003.11.076

The tetrasubstituted benzotriazole compounds based on **1** were prepared quite readily as shown in Scheme 1. Treatment of benzotriazole with benzyl bromide in the presence of NaH in DMF gave the 1-benzyl-1*H*-1,2,3-benzotriazole. Deprotonation of the latter with *n*-butyl lithium followed by sequential alkylation with the appropriate electrophiles gave either the mono- or bis-phenyldifluoromethylphosphonic acid (PDFMP) derivatives. The same reaction sequence can be applied to other heterocyclic benzylated benzotriazoles.

The ability of these compounds to inhibit PTP-1B was assessed with the fluorescein diphosphate (FDP) assay[12] and the PTP-1B overexpressed S*f*-9 cell assay.[13] The results are summarized in Tables 1–3.

The trisubstituted benzotriazole compound **1** is much less active as a PTP-1B inhibitor than the tetrasubstituted analogue **2** which differs by an extra bromobenzyl substituent in a tetrahedral arrangement. Varying the chain length of the lipophilic bromobenzyl substituent (**3**–**6**) has little effect on potency. A similar result was reported in the deoxybenzoin series. This indicates that the rigid tetrahedral orientation as well as the presence of all four substituents is essential for the increase in potency. However replacing the benzylic linkage with an ester renders the compound (**7**) less potent. Polar substituents such as sulfonamide and tetrazole (**8** and **9**) at the end of the lipophilic chain have no effect on the potency except when it is substituted by another difluoromethylphosphonic acid (**10**). Compound **10** is more potent than the exact analogue of the benzoin series with an IC_{50} = 0.016 μM in the PTP-1B assay. The compound is also active in the intact S*f*9 cell assay with an IC_{50} = 0.12 μM. The results suggest that the benzotriazole ring might have a more significant interaction with the enzyme at the active site. The ortho-bromo analogue **11** was even more potent with an IC_{50} = 0.005 μM. All

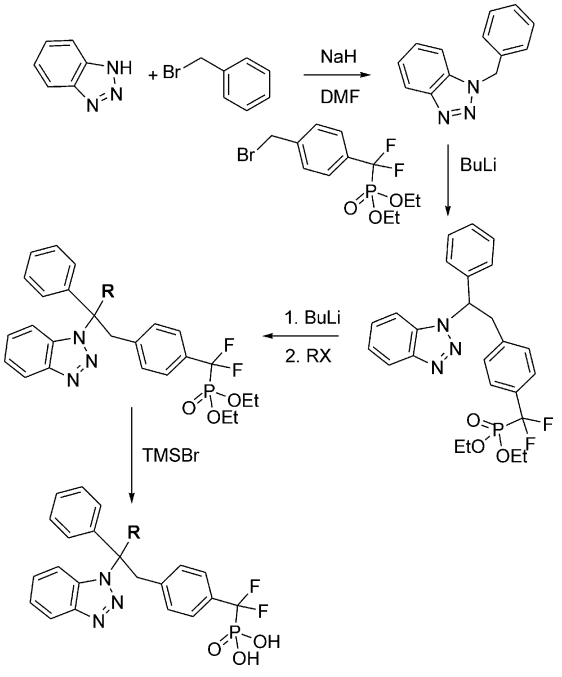

Scheme 1.

these compounds show excellent selectivity against other phosphatases such as CD-45 but not against TC-PTP (Table 1).

As noted earlier, the tetrahedral oriented scaffold facilitates the exploration of SAR in a wider area of space. Presumably, in this series of compounds, one of the phenyldifluoromethylphosphonic acids is anchored into the phosphate-binding loop of the active site of PTP-1B. The benzotriazole serves as a second anchor while the lipophilic chain provides lipophilic interaction with the enzyme. These three substituents are optimized for potency but not selectivity against TC-PTP. Attention was then turned to the study of the SAR of the remaining phenyl substituent. The results are summarized in Table 2.

Substitution of the phenyl ring with electron withdrawing or donating group has no effect on potency or selectivity against TC-PTP (examples **12**, **13**). Replacing the phenyl group with nitrogen bearing heterocycles (**14**–**17**) had no effect on potency or selectivity either while the benzothiazole **14**, tetrazole **16** and the phenylthiazole **17** have lost some selectivity against CD-45 (Table 2). Based on SAR at this juncture, the quest for selectivity against TC-PTP appeared futile. Fortunately, the X-ray crystal structure of PTP-1B complexed with compound **12** provided the crucial information on how this series of compounds binds to the active site. This allowed us to design selective compounds against TC-PTP based on the small difference between the two enzymes in the active site.

Figure 1 shows how compound **12** binds in the active site of PTP-1B. The phenyldifluoromethylphosphonate buried in the primary binding site is only partly visible, mostly obscured by the flap Phe182. The difluorophenyl makes weak interactions with the protein surface, while the benzotriazole makes a hydrogen bond to the peptide backbone between Arg47 and Asp48 (which make a salt bridge) as well as hydrophobic interactions with the Arg47 side-chain. A pathway to selectivity lay in the part of the active site that binds the other phenyldifluoromethylphosphonate. This fragment lies exposed on the surface with the phenyl ring lying in a shallow lipophilic shelf where the lipophilic chain of compounds **2**–**6** presumably also lie. The increased potency over the hydrogen substituted **1** can be attributed to this lipophilic interaction. The difluoromethylphosphonate moiety does not reach the two arginines (Arg24 andArg254) associated with the secondary phosphotyrosine (pY) binding site.[14] Based on sequence alignment of the highly-homologous PTP-1B and TC-PTP, there are only two amino acid residue differences between the two enzymes in the first shell of the active site, located at the periphery of the secondary binding site. Phenylalanine 52 (F52) and the alanine 27 (A27) in PTP-1B (both in yellow in Fig. 1) are replaced by a tyrosine and a serine respectively in TC-PTP.

Based on this information, molecular modeling suggested that extending the lipophilic chain to the secondary binding site could be achieved readily with a rigid biphenyl linker. Optimum binding to the two arginines (R24 and R254)

Table 1.

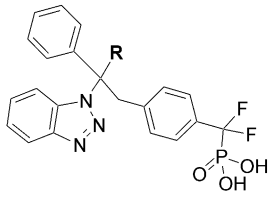

Compd	R	PTP-1B (IC_{50} μM)	CD-45 (IC_{50} μM)	TC-PTP (IC_{50} μM)	SF9 (IC_{50} μM)
1	H	8.04	> 50	7.26	—
2	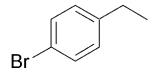	0.089	17	0.092	1.60
3	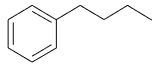	0.046	30	0.072	0.65
4	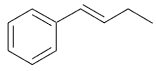	0.049	50	0.049	0.46
5	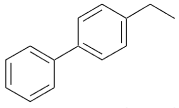	0.038	69	0.024	1.60
6	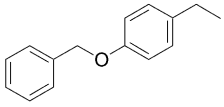	0.098	64	0.062	4.07
7	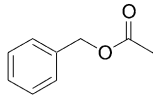	0.24	50	0.29	1.7
8	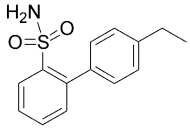	0.069	50	0.082	0.93
9	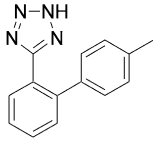	0.074	50	0.085	0.37
10	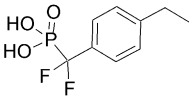	0.016	50	0.010	0.12
11	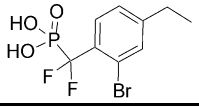	0.005	25	0.004	0.16

at the secondary binding site could be attained by placing a phosphonic acid at the meta-position of the terminal phenyl ring. With both phosphonic acids anchored into the primary and secondary binding site, and the benzotriazole to provide the third anchor, the molecule would be rigidly locked into the active site. Modeling suggested that with a rigid substituent, like that of a methylquinoline with disubstitution on the methyl substituent protruding towards the F52 (a slightly more bulky tyrosine in TC-PTP in this position), some selectivity could be obtained (Fig. 2). The biphenylphosphonic acid (**19**) was prepared and it was found to be the most potent PTP-1B inhibitor with an $IC_{50} = 0.003$ μM. The binding mode was confirmed by X-ray of the PTP-1B complexed with the compound. With the X-ray and modeled active sites superimposed based on active site Cαs, the X-ray inhibitor was within 1 Å RMSD from the modeled inhibitor, and both secondary phosphonate binding sites were occupied as predicted. The corresponding methylquinoline phosphonic acid **20**, providing the scaffolding for the designed selective compounds, was less potent. Both compounds were not selective against TC-PTP.

Table 2.

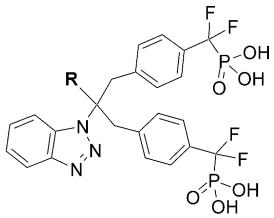

Compd	R	PTP-1B (IC_{50} μM)	CD-45 (IC_{50} μM)	TC-PTP (IC_{50} μM)	SF9 (IC_{50} μM)
12	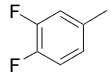	0.012	50	0.008	0.12
13	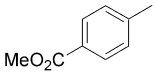	0.011	50	0.016	0.084
14	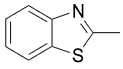	0.018	11	0.020	0.088
15	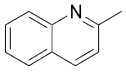	0.020	50	0.028	0.062
16		0.032	7.2	0.016	1.2
17	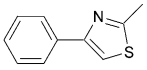	0.019	50	0.018	0.19

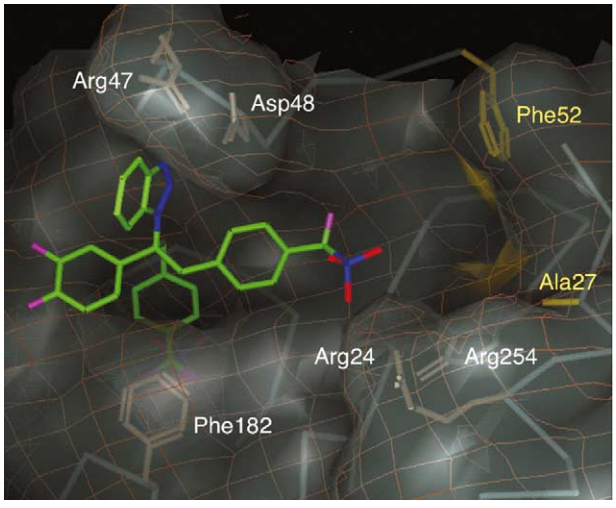

Figure 1. X-ray structure of compound **12** in the active site of PTP-1B. Active-site residues important for binding and conserved between PTP-1B and TC-PTP are labeled in white. The two active-site residues that differ between the two isoforms, Ala27 and Phe52, are depicted in yellow, with the exposed active site surface of these residues also in yellow.

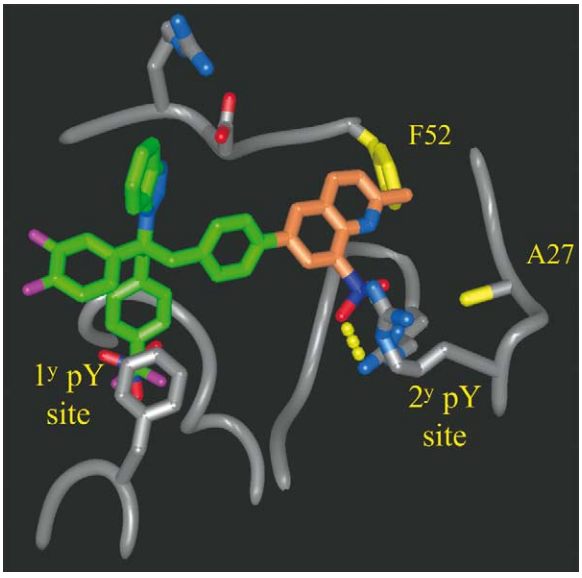

Figure 2. Compound **20** modeled into PTP-1B. The ligand parent scaffold is in green, the designed methylquinolinephosphonate fragment is in orange. Compared to compound **12**, the second phosphonate is positioned to take advantage of the two arginines in the secondary binding site (Arg24 and Arg254, see Fig. 1), and the methyl is poised close to Phe52 so that substitution on the methyl will introduce selectivity against TC-PTP.

However, disubstituting the methyl by making the methoxyisobutylquinoline analogue **21** showed moderate selectivity. The four diastereomers of **21** were resolved. The most potent isomer **21a** has an $IC_{50} = 0.005$ μM in the PTP-1B enzyme assay and an $IC_{50} = 0.036$ μM in the TC-PTP assay. The X-ray structure of PTP-1B complexed with this isomer has been obtained and the predicted structure was confirmed (Fig. 3).

The slightly less potent diastereomer **21b** with an $IC_{50} = 0.007$ μM in the PTP-1B enzyme assay and an $IC_{50} = 0.041$ μM in the TC-PTP assay is presumed to be isomeric at the methoxybutyl side chain of the quinoline.

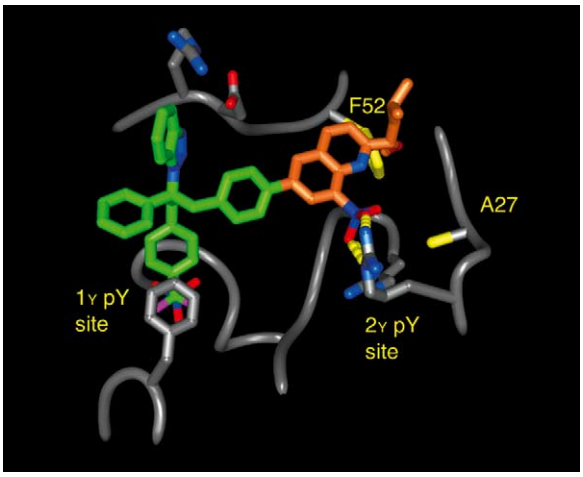

Figure 3. X-ray structure of compound **21a** in the active site of PTP-1B. With a virtually identical binding mode to that predicted for compound **20** (see Fig. 2), the introduction of the methoxy and isobutyl substituents on the methylquinoline forced an interaction with Phe52 in PTP-1B but which was less tolerated by the larger Tyr at this position in TC-PTP, leading to modest selectivity against TC-PTP.

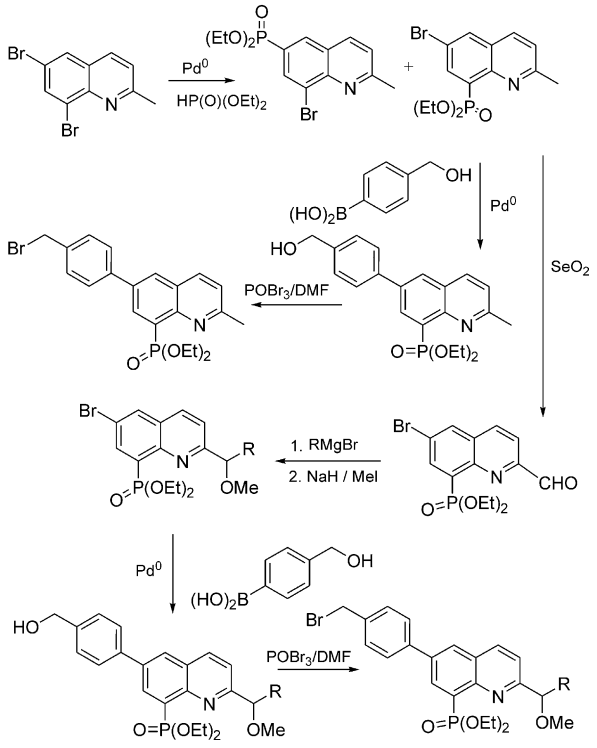

Scheme 2.

Table 3.

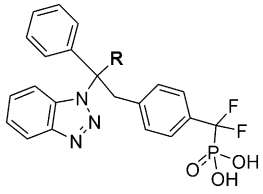

Compd	R	PTP-1B (IC_{50} μM)	CD-45 (IC_{50} μM)	TC-PTP (IC_{50} μM)	SF9 (IC_{50} μM)
10	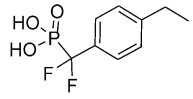	0.016	50	0.010	0.12
18	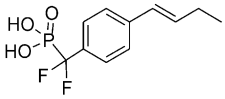	0.016	50	0.010	0.12
19	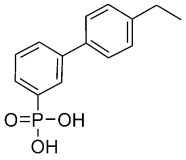	0.003	50	0.003	0.24
20	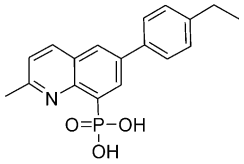	0.012	50	0.020	0.22
21a	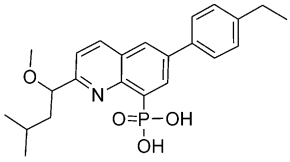	0.005	50	0.036	0.058
21b		0.007	50	0.041	0.10
21c		0.28	50	1.13	5.34
21d		0.20	32	0.93	1.79

Since the other two diastereomers are much less potent, it is reasonable to assume that they are isomeric at the methine where the benzotriazole and the difluorophenyl group switched position. The result provides an estimate on how much binding energy the benzotriazole nitrogen provides. The results are summarized in Table 3. The quinoline derivatives are prepared from 6,8-dibromo-2-methylquinoline using standard Suzuki coupling reactions and simple functional group transformations as shown in Scheme 2.

In summary, structure based design has provided a series of very potent PTP-1B inhibitors. Moderate selectivity against TC-PTP can be obtained by design.

References and notes

1. Bandyopadhyay, D.; Kusari, A.; Kenner, K. A.; Liu, F.; Chernoff, J.; Gustafson, T. A.; Kusari, J. *J. Biol. Chem.* **1997**, *272*, 1639.
2. Kenner, K. A.; Anyanwu, E.; Olefsky, J. M.; Kusari, J. *J. Biol. Chem.* **1996**, *271*, 19810.
3. Ahmad, F.; Li, P. M.; Meyerovitch, J.; Goldstein, B. J. *J. Biol. Chem.* **1995**, *270*, 20503.
4. Elchebly, M.; Payette, P.; Michaliszyn, E.; Cromlish, W.; Collins, S.; Loy, A. L.; Normandin, D.; Cheng, A.; Himms-Hagen, J.; Chan, C. C.; Ramachandran, C.; Gresser, M. J.; Tremblay, M. L.; Kennedy, B. P. *Science (Washington, D.C.)* **1999**, *283*, 1544.
5. Ahmad, F.; Considine, R. V.; Goldstein, B. J. *J. Clin. Invest.* **1995**, *95*, 2806.
6. Ahmad, F.; Azevedo, J. L.; Cortright, R.; Dohm, G. L.; Goldstein, B. J. *J. Clin. Invest.* **1997**, *100*, 449.
7. Kusari, J.; Kenner, K. A.; Suh, K. I.; Hill, D. E.; Henry, R. R. *J. Clin. Invest.* **1994**, *93*, 1156.
8. Zinker, B. A.; Rondinone, C. M.; Trevillyan, J. M.; Gum, R. J.; Clampit, J. E.; Waring, J. F.; Xie, N.; Wilcox, D.; Jacobson, P.; Frost, L.; Kroeger, P. E.; Reilly, R. M.; Koterski, S.; Opgenorth, T. J.; Ulrich, R. G.; Crosby, S.; Butler, M.; Murray, S. F.; McKay, R. A.; Bhanot, S.; Monia, B. P.; Jirousek, M. R. *Proc. Natl. Acad. Sci. U.S.A* **2002**, *99*, 11357.
9. Kennedy, B. P.; Ramachandran, C. *Biochem. Pharmacol.* **2000**, *60*, 877.
10. Johnson, T. O.; Ermolieff, J.; Jirousek, M. R. *Nat. Rev. Drug Discov.* **2002**, *1*, 696.
11. You, T.; Muise, E. S.; Itie, A.; Michaliszyn, E.; Wagner, J.; Jothy, S.; Lapp, W. S.; Tremblay, M. L. *J. Exp. Med.* **1997**, *186*, 683.
12. Huang, Z.; Wang, Q.; Ly, H. D.; Gorvindarajan, A.; Scheigetz, J.; Zamboni, R.; Desmarais, S.; Ramachandran, C. *J. Biomol. Screen.* **1999**, *4*, 327.
13. Cromlish, W. A.; Payette, P.; Kennedy, B. P. *Biochem. Pharmacol.* **1999**, *58*, 1539.
14. Puius, Y. A.; Zhao, Y.; Sullivan, M.; Lawrence, D. S.; Almo, S. C.; Zhang, Z. Y. *Proc. Natl. Acad. Sci. U.S.A.* **1997**, *94*, 13420.